Design of a new type of fly-back nonmetal ultrasonic generating circuit

Chao Peng[1,*], Yue Song[1], Leshuang Zhou[1], Sha Zou[2]

[1]School of Electrical Engineering and Intelligentization, Dongguan University of Technology, Dongguan, 523808, China

[2]School of Hengnan County seventh middle, Hengyang, 421000, China

*E-mail: pengchao@dgut.edu.cn

Keywords: Double core system;Flyback ultrasonic emission; non-metal; Ultrasonic examination

Abstract: In this paper, a new type of non-metallic ultrasonic transmitting circuit is designed. This circuit uses the principle of flyback pulse excitation, The charging and discharging time of RC circuit is controlled by a frequency adjustable pulse output from Double core system, so that the transmitting voltage and radio frequency rate can be adjusted flexibly. By establishing the circuit model of the ultrasonic transmitting circuit and making the actual circuit, it is proved that the circuit can generate the ultrasonic pulse excitation signal with adjustable frequency and amplitude, thus improving the common problem that the transmitting efficiency of the probe in the traditional circuit is lower than the actual one, and improving the transmitting efficiency of the probe. Finally, the experiment was verified and the effect was good.

1. Introduction

Ultrasound transmitting circuit is an important part of the ultrasonic flaw detector. The accuracy and stability of this part are very important to the whole ultrasonic flaw detection system[1, 2]. The transmitting circuit of non-metallic flaw detection completes the excitation of ultrasonic pulse signal. The excitation energy mainly depends on the voltage applied on the two ends of the transducer. Therefore, in order to obtain enough energy, it is necessary to generate enough high-voltage pulse. Most of the high-voltage pulse generation uses the capacitor instantaneous discharge method, which uses the property that the voltage across the capacitor cannot be abruptly changed, and generates a high-voltage pulse through the charge and discharge of the capacitor. This method has a simple circuit and low electrical losses, but requires DC high voltage. The DC high voltage is usually based on the principle of DC inversion, which generates oscillation signal, high voltage alternating current after transforming voltage, and then rectifier filter to get DC high voltage. so that the circuit is generally bulky, has many components, and has high cost[3].

This paper provides a stable DC high voltage for the capacitor transient transmitting circuit, while reducing the size of the circuit and improving the stability of the circuit. In the capacitance instantaneous transmission circuit, the design of the paper improves the common problem that the probe emission efficiency in the traditional circuit is lower than the actual problem, and improves the probe emission efficiency.

2. The overall design of ultrasonic transmitting circuit

The system block diagram of the non-metallic ultrasonic emission circuit is shown in Figure 1. This design consists of four main components: ARM + FPGA dual core control system, DC high voltage power supply and improved capacitor instantaneous transmission circuit.

  DOI: 10.25236/eeems.2018.006

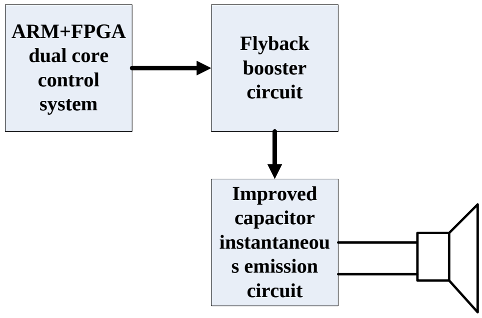

Figure 1 The system block diagram

Among them, the dual-core control system of ARM + FPGA not only meets the requirements of control accuracy, but also meets the requirements of functional diversity in the future, and also lays the foundation for the expansion of the system in the future[4].

(1)The Design of DC high voltage power supply

In order to improve the power consumption of the high-voltage power supply and reduce the size and cost of the power supply, the DC high-voltage power supply adopts a flyback boost circuit design[5, 6]. A small integrated high voltage power module can reduce the development time[7]. In this design, we use LT3757 chip, which is a DC/DC controller with wide input voltage range and current mode. The device is capable of generating a positive or negative output voltage. It can be configured as a boost, buck, flyback, or SEPIC mode by configuring an external circuit. Here we use a flyback design. In the design, LT3757 chip is used to control duty cycle of flyback transformer to produce a stable 500V DC high voltage. The specific schematic diagram is shown in Figure 2.

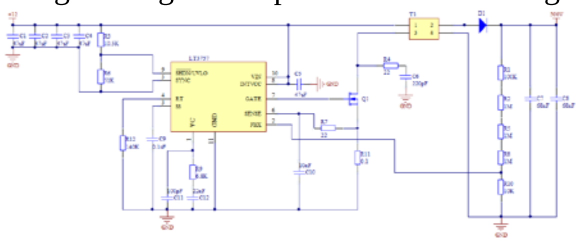

Figure 2 Flyback booster circuit

The circuit includes LT3757DC control chip, capacitor C1-C12, resistor R1-R11, rectifier diode D1, flyback transformer T1, N channel enhanced power field effect transistor Q1. By boosting the input 5V signal in the chip, 7.5V voltage is generated, which drives the Q1 switch of Mos tube, generates AC signal, drives the high frequency transformer to work, and outputs a 500V AC voltage. Finally, through the high voltage rectifier, 500V DC voltage is output.Here, pin 2 (FBX) of LT3757 is a positive and negative feedback pin. The external output voltage divider resistor receives the feedback voltage. When the chip starts the modulation frequency and an error occurs, the pin is close to ground potential.

(2) The Design of improved capacitor instantaneous transmitting circuit

The specific circuit is shown in Figure 3. The circuit includes electrolytic capacitor C4,bridge driver TC4420, N-channel enhanced power field effect transistor Q1, capacitor C1, C2, C3, switching diode D1, D2 and resistors R1, R2, R3, R4 R5, R6. The whole circuit uses the charge and discharge of the capacitor C1 to excite the ultrasonic probe, wherein the capacitor C2 is a compensation capacitor. The emission efficiency of an ultrasonic probe is mainly determined by the amplitude and frequency of the negative pulse voltage applied across the probe. When the excitation voltage is constant, the transmission efficiency is the highest when the frequency of the negative pulse voltage added to the probe is equal to or close to the frequency of the probe resonance. Since the actual resonant frequency of the ultrasonic transmitting probe is often smaller than the nominal frequency, the result of the received signal will eventually be unsatisfactory, so the compensation capacitor C2 is added for compensation to improve the transmission efficiency.

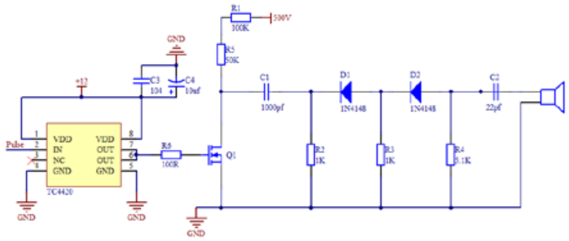

Figure 3 Improved capacitor instantaneous emission circuit

3. Calculation of compensation capacitance

The calculation of the compensation capacitor C2 is as follows: First, the equivalent circuit diagram of the ultrasonic probe is as shown in FIG. 4.

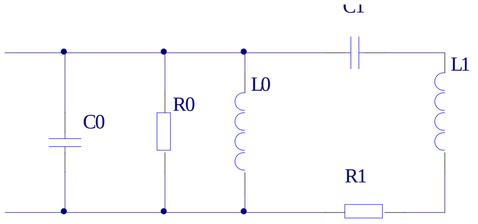

Figure 4 Equivalent circuit diagram of ultrasonic probe

Among them, C0, R0 and L0 are static branch equivalent circuits, and C1, R1 and L1 are dynamic branch circuit diagrams. The value of L0 of the static branch is generally very small, this can be ignored[8, 9], the same C0, R0 can be obtained through the specification of the probe. The dynamic characteristics C1, L1 and R1 can be obtained by the RLC meter[10]. With the parameters of dynamic circuit and static circuit, we can calculate the compensation capacitance by the following formula:

$$
\begin{aligned}
C_t &= \frac{A_3^2 + A_4^2}{\omega(A_2A_3 - A_1A_4)} \\
A_1 &= \omega^3 R_0^2 C_0 C_1 L_1 + \omega R_0 R_1 C_1 - \omega R_0^2 C_0 \\
A_2 &= \omega^2 R_0 C_1 L_1 - \omega^2 R_0^2 C_0 C_1 R_1 - R_0 \\
A_3 &= \omega^3 R_0^2 C_0^2 C_1 R_1 + \omega R_1 C_1 + \omega R_0 C_1 \\
A_4 &= \omega^4 R_0^2 C_0^2 C_1 L + \omega^2 C_1 L_1 - \omega^2 R_0^2 C_0^2 - \omega^2 R_0^2 C_0 C_1 - 1
\end{aligned}
\qquad (1)
$$

The circuit of Figure 3 adds the compensation capacitor C2 to match the probe. By matching the equivalent circuit of the probe, the frequency of the negative pulse voltage applied to the probe is equal to or close to the resonant frequency of the probe, thereby effectively improving the emission efficiency of the probe[11, 12].

4. Experimental test

After theoretically designing the circuit, we use PROTEL to simulate the whole circuit into a compact printed circuit board, and then make it into a physical object, as shown in Fig. 5.

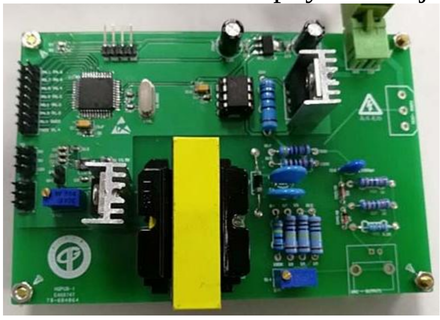

Figure 5 Physical map of the transmitting circuit

Then we tested the circuit. The test results are shown in Figure 6.

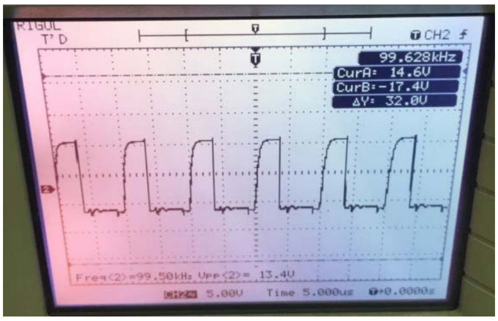

Figure 6 Excitation pulse waveform during test

From the test results, the output waveform of the transmitting circuit is stable, the frequency is adjustable, and the pulse width and the excitation narrow pulse are in line with the engineering requirements of ultrasonic flaw detection [13]. At the same time, we test the compensation capacitance. We detect the corresponding echo amplitude according to different compensation capacitance values. The experimental results are shown in Table 1.

Table 1 The experimental data of the echo amplitude corresponding to the theoretical value of the compensation capacitor C2=0.02 μf .

Actual value of C2/ μf	Nominal frequency/KHz	Echo frequency/KHz	Echo amplitude/mV
0	100	100	60
0.015	100	100	192
0.022	100	100	378
0.05	100	100	316
0.1	100	100	200
0.22	100	100	95

From Table 1, it can be seen that when the compensation capacitance changes from small to large, the closer the real value of the compensation capacitance is to the theoretical value, the larger the echo amplitude is. When the true value of the compensation capacitor exceeds the theoretical value, the amplitude of the echo gradually decreases. When the amplitude is the highest, it indicates that the received energy is the most, and the emission efficiency is the highest. This set of experimental data verifies the correctness of the theoretical calculation of the compensation capacitance according to Equation 1.We can calculate the compensation capacitance quickly according to the theoretical formula, so that the emission efficiency can be optimized.

5. Conclusions

Compared with the traditional capacitor instantaneous discharge method, this paper uses a new type of flyback boosting method to provide a stable DC high voltage for the capacitor instantaneous transmitting circuit, while reducing the volume of the circuit and improving the stability of the circuit. In the capacitor instantaneous transmitting circuit, this paper quickly calculates the size of the compensation capacitor by calculating the compensation capacitor in a theoretical way, Thus improving the efficiency of the probe emission is lower than the actual problem, which greatly improves the efficiency of the probe. The research in this paper can provide technical support and theoretical guidance for ultrasonic nondestructive testing[14, 15], and has certain engineering value.

Acknowledgments

This work was supported by Dongguan Municipal Science and Technology Bureau under grant No. 2016508140.

References

[1] Park, J.B., Y.J. Jang, B.K. Choi, K.K. Kim, and Y. Ko, Treatment with various ultrasonic scaler tips affects efficiency of brushing of SLA titanium discs. J Craniofac Surg, 2013. 24(2): p. e119-23.

[2] Pipa, A.V., T. Hoder, J. Koskulics, M. Schmidt, and R. Brandenburg, Experimental determination of dielectric barrier discharge capacitance. Rev Sci Instrum, 2012. 83(7): p. 075111.

[3] Olcum, S., F.Y. Yamaner, A. Bozkurt, H. Koymen, and A. Atalar, An equivalent circuit model for transmitting capacitive micromachined ultrasonic transducers in collapse mode. IEEE Trans Ultrason Ferroelectr Freq Control, 2011. 58(7): p. 1468-77.

[4] Song, Y., J.A. Turner, Z. Peng, C. Chen, and X. Li, Enhanced Ultrasonic Flaw Detection Using an Ultrahigh Gain and Time-Dependent Threshold. IEEE Trans Ultrason Ferroelectr Freq Control, 2018. 65(7): p. 1214-1225.

[5] Coutinho, F.R., C.Y. Ofuchi, L.V. de Arruda, F.J. Neves, and R.E. Morales, A new method for ultrasound detection of interfacial position in gas-liquid two-phase flow. Sensors (Basel), 2014. 14(5): p. 9093-116.

[6] Liu, L., J. Wen, Y. Yang, and W. Tan, Ultrasound field distribution and ultrasonic oxidation desulfurization efficiency. Ultrason Sonochem, 2013. 20(2): p. 696-702.

[7] Hao, L., R. Wang, K. Fang, and J. Liu, Ultrasonic effect on the desizing efficiency of alpha-amylase on starch-sized cotton fabrics. Carbohydr Polym, 2013. 96(2): p. 474-80.

[8] Li, W., T. Leong, M. Ashokkumar, and G. Martin, A study of the effectiveness and energy efficiency of ultrasonic emulsification. Phys Chem Chem Phys, 2017. 20(1): p. 86-96.

[9] Benammar, A., R. Drai and A. Guessoum, Ultrasonic flaw detection using threshold modified S-transform. Ultrasonics, 2014. 54(2): p. 676-83.

[10] Mu, J., X. Chou, Z. Ma, J. He, and J. Xiong, High-Performance MIM Capacitors for a Secondary Power Supply Application. Micromachines (Basel), 2018. 9(2).

[11] Lee, B.C., A. Nikoozadeh, K.K. Park, and B.T. Khuri-Yakub, High-Efficiency Output Pressure Performance Using Capacitive Micromachined Ultrasonic Transducers with Substrate-Embedded Springs. Sensors (Basel), 2018. 18(8).

[12] Bandelin, J., T. Lippert, J.E. Drewes, and K. Koch, Cavitation field analysis for an increased efficiency of ultrasonic sludge pre-treatment using a novel hydrophone system. Ultrason Sonochem, 2018. 42: p. 672-678.

[13] Radosz, J. and D. Pleban, Ultrasonic noise measurements in the work environment. J Acoust Soc Am, 2018. 144(4): p. 2532.

[14] Liu, W., Y. Tan, Z. Gao, S. Chai, and S. Hong, A low noise power supply based on buck converter for current regulation in an inductive load. Rev Sci Instrum, 2018. 89(10): p. 10K115.

[15] Zhang, G., J. Zhu, Y. Song, C. Peng, and G. Song, A Time Reversal Based Pipeline Leakage Localization Method With the Adjustable Resolution. IEEE Access, 2018. 6; 6: p. 26993-27000.